Glycobiology vol. 23 no. 3 pp. 381–394, 2013
doi:10.1093/glycob/cws166
Advance Access publication on December 18, 2012

KSGal6ST generates galactose-6-*O*-sulfate in high endothelial venules but does not contribute to L-selectin-dependent lymphocyte homing

Michael L Patnode[2], Shin-Yi Yu[3,4], Chu-Wen Cheng[3], Ming-Yi Ho[3], Lotten Tegesjö[2], Keiichiro Sakuma[5], Kenji Uchimura[6], Kay-Hooi Khoo[3], Reiji Kannagi[4,5], and Steven D Rosen[2,1]

[2]Department of Anatomy and Program in Biomedical Sciences, University of California, San Francisco, CA 94143-0452, USA; [3]Institute of Biological Chemistry, and [4]Institute of Biomedical Sciences, Academia Sinica, Taipei 11529, Taiwan; [5]Division of Molecular Pathology, Aichi Cancer Center, Nagoya 464-8681, Japan; and [6]Department of Biochemistry, Nagoya University, Graduate School of Medicine, Aichi 466-8550, Japan

Received on October 25, 2012; revised on November 30, 2012; accepted on November 30, 2012

The addition of sulfate to glycan structures can regulate their ability to serve as ligands for glycan-binding proteins. Although sulfate groups present on the monosaccharides glucosamine, uronate, *N*-acetylglucosamine and *N*-acetylgalactosamine are recognized by defined receptors that mediate important functions, the functional significance of galactose-6-*O*-sulfate (Gal6S) is not known. However, in vitro studies using synthetic glycans and sulfotransferase overexpression implicate Gal6S as a binding determinant for the lymphocyte homing receptor, L-selectin. Only two sulfotransferases have been shown to generate Gal6S, namely keratan sulfate galactose 6-*O*-sulfotransferase (KSGal6ST) and chondroitin 6-*O*-sulfotransferase-1 (C6ST-1). In the present study, we use mice deficient in KSGal6ST and C6ST-1 to test whether Gal6S contributes to ligand recognition by L-selectin in vivo. First, we establish that KSGal6ST is selectively expressed in high endothelial venules (HEVs) in lymph nodes and Peyer's patches. We also determine by mass spectrometry that KSGal6ST generates Gal6S on several classes of O-glycans in peripheral lymph nodes. Furthermore, KSGal6ST, but not C6ST-1, is required for the generation of the Gal6S-containing glycan, 6,6′-disulfo-3′sLN (Siaα2→3[6S]Galβ1→4[6S]GlcNAc) or a closely related structure in lymph node HEVs. Nevertheless, L-selectin-dependent short-term homing of lymphocytes is normal in KSGal6ST-deficient mice, indicating that the Gal6S-containing structures we detected do not contribute to L-selectin ligand recognition in this setting. These results refine our understanding of the biological ligands for L-selectin and introduce a mouse model for investigating the functions of Gal6S in other contexts.

Keywords: galactose-6-*O*-sulfate / keratan sulfate / L-selectin / lymphocyte homing / sulfotransferase

Introduction

The attachment of sulfate esters to biomolecules is essential for development, survival and reproduction in animals (Borghei et al. 2006; Bulow and Hobert 2006). The diverse functions of carbohydrate sulfation reflect the diverse glycan substrates to which sulfate can be added (Khoo and Yu 2010). Precise positioning of sulfate on these glycans determines whether they serve as ligands for one or more glycan-binding proteins. Heparan sulfate proteoglycans (HSPGs) provide a clear demonstration of these principles, since they carry long carbohydrate chains with variable sulfate modifications, including *N*-acetylglucosamine-6-*O*-sulfate (GlcNAc6S), *N*-acetylglucosamine-3-*O*-sulfate, glucosamine-*N*-sulfate and uronate-2-*O*-sulfate (Bishop et al. 2007). These modifications dictate the binding of HSPGs to numerous growth factors, apolipoproteins and lipases, cell adhesion molecules and extracellular matrix components (Bishop et al. 2007). Sulfate modifications on smaller glycans carried by glycoproteins and glycolipids also serve important functions. *N*-acetylgalactosamine-4-*O*-sulfate, which caps N-glycan chains on several glycoprotein hormones, is required for their recognition by the macrophage mannose receptor and efficient clearance from the circulation (Baenziger 2003). Galactose-3-*O*-sulfate (Gal3S) is present on the glycolipids seminolipid and sulfatide and is essential for spermatogenesis and normal myelin function (Honke et al. 2004). In contrast, the functions of galactose-6-*O*-sulfate (Gal6S) have not been established. However, this modification has been implicated as a binding determinant for several immunologically relevant receptors (Bochner et al. 2005; Tateno et al. 2005, 2010; Campanero-Rhodes et al. 2006) including L-selectin, the focus of the present study.

L-selectin is a cell surface C-type lectin receptor constitutively expressed on nearly all circulating leukocytes (Butcher and Picker 1996). This receptor mediates transient adhesive

[1]To whom correspondence should be addressed: Tel: +1-415-476-1579; Fax: +1-415-476-4845; e-mail: steven.rosen@ucsf.edu

interactions between lymphocytes and specialized postcapillary venules in lymph nodes known as high endothelial venules (HEVs), which are characterized by their plump endothelial cells. The relatively weak affinity of these interactions, combined with the shear force of blood flow, causes lymphocytes to roll along the walls of HEVs. Lymphocyte rolling, in turn, enables integrin-mediated arrest to take place, which precedes the exit of lymphocytes from the bloodstream into the tissue (Ley et al. 2007). Thus, L-selectin ligands expressed by HEVs are critically involved in the process of lymphocyte homing, which brings circulating lymphocytes into contact with antigens to generate immune responses. Several mucin scaffolds expressed by HEVs have been identified as ligands for L-selectin, including GlyCAM-1, CD34, endomucin, podocalyxin and nepmucin (Rosen 2004). These ligands present terminal oligosaccharides that are bound by L-selectin, the best characterized of which is 6-sulfo-sLex (Siaα2→3Galβ1→4[Fucα1→3][6S]GlcNAc) (Hemmerich et al. 1995; Mitsuoka et al. 1998). Antibodies recognizing this structure stain HEVs in human and mouse lymph nodes, and block L-selectin function (Mitsuoka et al. 1998; Hirakawa et al. 2010; Arata-Kawai et al. 2011). Accordingly, structures consistent with 6-sulfo-sLex have been detected on human CD34 by mass spectrometry (MS) (Satomaa et al. 2002; Hernandez Mir et al. 2009). The critical contributions of fucose and sialic acid (Sia) to the 6-sulfo-sLex-binding determinant have been demonstrated with mice deficient in α3-fucosyltransferases (FucT-IV and FucT-VII) (Homeister et al. 2001) or α3-sialyltransferases (ST3Gal-IV and ST3Gal-VI) (Yang et al. 2012). Similarly, mice lacking the core 2 (Core2GlcNAcT) and core 1 extensions (β3GlcNAcT-3) enzymes have illustrated the significance of 6-sulfo-sLex capping groups on each of these O-glycan arms, and revealed that N-glycans capped with 6-sulfo-sLex also contribute to lymphocyte homing (Mitoma et al. 2007). Importantly, 6-sulfo-sLex carries the sulfate modification GlcNAc6S, which is required for optimal binding by L-selectin (Rosen 2004).

Carbohydrate sulfation is dictated by the expression of sulfotransferases, enzymes that catalyze the transfer of sulfate from the universal donor 3′-phospho-adenosine-5′-phosphosulfate (PAPS) to specific hydroxyl or amino groups on nascent glycans in the Golgi network (Grunwell and Bertozzi 2002). The *N*-Acetylglucosamine-6-*O*-sulfotransferases GlcNAc6ST-1 (encoded by the gene *Chst2*) and GlcNAc6ST-2 (encoded by the gene *Chst4*) generate nearly all of the 6-sulfo-sLex in HEVs (Kawashima et al. 2005; Uchimura et al. 2005). We and others have shown that GlcNAc6ST-1/GlcNAc6ST-2 double-knockout (GlcNAc6ST1/2 DKO) mice exhibit a 75% decrease in lymphocyte homing to peripheral lymph nodes (PLN) (Kawashima et al. 2005; Uchimura et al. 2005). Interestingly, the residual homing in these mice is L-selectin-dependent and, therefore, indicates the presence of alternative recognition determinants that can substitute for GlcNAc6S. In fact, several lines of evidence have suggested that Gal6S contributes to L-selectin-dependent lymphocyte homing. First, Gal6S and GlcNAc6S were found in approximately equal abundance on mouse GlyCAM-1 and CD34 by anion exchange chromatography of monosaccharides released by mild acid hydrolysis (Hemmerich et al. 1994; Bistrup et al. 1999). Based on structural analysis of the O-glycans of GlyCAM-1, Hemmerich et al. (1995) proposed the existence of 6′-sulfo-sLex (Siaα2→3[6S]Galβ1→4[Fucα1→3]GlcNAc), as well as 6-sulfo-sLex. However, with respect to the former structure, it has subsequently been appreciated that the addition of sulfate to the 6-*O* position of galactose (Gal) and the addition of α3-linked fucose on GlcNAc appear to be mutually exclusive within the same *N*-acetyllactosamine (LacNAc, Galβ1→4GlcNAc) unit in vivo (Torii et al. 2000; Homeister et al. 2001; Hiraoka et al. 2007). Indeed, 6′-sulfo-sLex was not found in GlyCAM-1 O-glycans analyzed by high-performance liquid chromatography (HPLC), although Gal6S was present at the termini of core 1 and core 2 arms (Kawashima et al. 2005; Hiraoka et al. 2007). The artificial addition of sulfate to 6-*O* position of Gal within sLex only marginally enhances (Koenig et al. 1997), and can even inhibit, the binding of sLex to L-selectin-Fc fusion proteins (Galustian et al. 1997; Yoshino et al. 1997). However, Gal6S has been implicated as a binding determinant for L-selectin when present on structures other than sLex. When lactose (Galβ1→4Glc) neoglycolipids were synthesized with sulfate on the 6-*O* position of Gal, they exhibited binding to L-selectin-Fc and L-selectin-expressing Jurkat T cells (Bruehl et al. 2000). Furthermore, 6,6′-disulfo-lactose ([6S]Galβ1→4[6S]Glc) showed even more binding in these assays than either singly sulfated lactose, and also preferentially inhibited the binding of L-selectin-Fc to GlyCAM-1 (Bertozzi et al. 1995). These observations raise the possibility that fucose and Gal6S in distinct LacNAc units can cooperate with GlcNAc6S for recognition by L-selectin.

Additional evidence implicating Gal6S as a binding determinant for L-selectin has come from studies of keratan sulfate galactose 6-*O*-sulfotransferase (KSGal6ST, encoded by the gene *Chst1*). Biochemical characterization of this sulfotransferase has established that it catalyzes 6-*O* sulfation of Gal in keratan sulfate (KS) chains (Fukuta et al. 1997), which consist of repeating 6-sulfo-LacNAc (Galβ1→4[6S]GlcNAc) units intermittently modified with Gal6S (Bulow and Hobert 2006). However, in vitro studies have shown that KSGal6ST is also capable of modifying Gal in small sialylated lactosamine oligosaccharides, such as 3′sLN (Siaα2→3Galβ1→4GlcNAc) (Torii et al. 2000), which are present on the O-glycans of mucins expressed by HEVs. Indeed, we previously demonstrated that KSGal6ST can add sulfate to GlyCAM-1 when both genes, along with FucT-VII and Core2GlcNAcT, are transiently overexpressed in COS-7 cells (Bistrup et al. 1999). Furthermore, this form of GlyCAM-1 was a superior substratum for lymphocyte rolling when compared with GlyCAM-1 produced without KSGal6ST overexpression (Tangemann et al. 1999). Similarly, transient overexpression of KSGal6ST, CD34, FucT-VII and Core2GlcNAcT in Chinese hamster ovary (CHO) cells resulted in increased cell-surface binding of L-selectin-Fc relative to cells not overexpressing KSGal6ST (Bistrup et al. 1999). Intriguingly, KSGal6ST and GlcNAc6ST-2 had synergistic effects on L-selectin binding in this study, reminiscent of the synergy between Gal6S and GlcNAc6S within lactose neoglycolipids. Finally, stable overexpression of KSGal6ST, along with FucT-VII, in an

endothelial cell monolayer increased its ability to support the rolling of L-selectin-expressing lymphoma cells (Li et al. 2001). All of these studies were performed with expression of FucT-VII, demonstrating that Gal6S can contribute to L-selectin ligand activity even in the presence of α3-linked fucose on GlcNAc. Additionally, KSGal6ST was at least as effective as either GlcNAc6ST-1 or GlcNAc6ST-2 in generating L-selectin ligand activity. However, the effects of Gal6S appear to depend on the exact experimental conditions, since another study found that transient overexpression of KSGal6ST in CHO cells stably expressing CD34, FucT-VII and GlcNAc6ST-1, actually reduced their ability to support lymphocyte rolling (Hiraoka et al. 2007).

Aside from KSGal6ST, only one other sulfotransferase has been shown to generate Gal6S, namely chondroitin 6-*O*-sulfotransferase-1 (C6ST-1, encoded by the gene *Chst3*). This sulfotransferase is less likely to participate in generating L-selectin ligands for several reasons. C6ST-1 exhibits 5-fold more GalNAc-6-*O*-sulfotransferase activity than Gal-6-*O*-sulfotransferase activity in vitro (Habuchi et al. 1996), and it has been shown to function in the synthesis of chondroitin sulfate, but not KS in vivo (Uchimura et al. 2002). Furthermore, C6ST-1 catalyzes 6-*O* sulfation of Gal on small sialylated oligosaccharides almost 100-fold slower than it does on extended KS chains, whereas KSGal6ST has the opposite preference (Habuchi et al. 1997). Most pertinently, C6ST-1-deficient mice do not exhibit defects in lymphocyte homing (Uchimura et al. 2002).

In contrast to C6ST-1, KSGal6ST has not been previously investigated with respect to its capacity to generate Gal6S in vivo or its functional contribution to lymphocyte homing. Here, we report that KSGal6ST is selectively expressed in lymph node HEVs and generates Gal6S-containing glycans in lymph nodes, including 6,6′-disulfo-3′sLN (Siaα2→3[6S]Galβ1→4[6S]GlcNAc) or a closely related structure in HEVs. However, using KSGal6ST KO mice, we find that the Gal6S-containing structures we detected do not contribute to normal L-selectin-dependent short-term lymphocyte homing, or to the residual homing seen in the absence of both GlcNAc6ST-1 and GlcNAc6ST-2.

Results

Generation of KSGal6ST-deficient mice

In order to study the functions of KSGal6ST in vivo, we obtained heterozygous mice carrying a targeted allele of *Chst1* from the National Institutes of Health Knockout Mouse Project. The targeted allele contains the *Escherichia coli* K-12 LacZ gene and a neomycin resistance cassette, which replace the single protein-coding region of *Chst1* (Figure 1A) (Valenzuela et al. 2003). We intercrossed mice heterozygous for this allele ($Chst1^{+/-}$ mice) to produce homozygous mice ($Chst1^{-/-}$ mice). Seven litters from $Chst1^{+/-} \times Chst1^{+/-}$ crosses yielded in total 12 $Chst1^{+/+}$, 26 $Chst^{+/-}$ and 12 $Chst1^{-/-}$ pups, consistent with the expected Mendelian frequencies. We observed no gross physical or behavioral abnormalities in $Chst1^{-/-}$ mice, except that male siblings housed together seemed particularly prone to fighting. Since *Chst1* is highly expressed in the cerebral cortex (www.biogps.org, GeneAtlas MOE430 probeset 1449147_at, GeneAtlas U133A probeset 205567_at) (Su et al. 2004), we performed reverse transcriptase (RT) polymerase chain reaction (PCR) on total RNA from whole forebrain and verified the absence of *Chst1* transcripts in $Chst1^{-/-}$ animals (Figure 1B).

Chst1 is also expressed in the eye (Su et al. 2004), along with KS chains containing Gal6S (Bhavanandan and Meyer 1967). Furthermore, KS is a known substrate for KSGal6ST (Fukuta et al. 1997), although this enzyme has not previously been shown to generate Gal6S in vivo. To determine whether KSGal6ST deficiency in $Chst1^{-/-}$ mice affects the sulfation pattern of KS, we isolated KS from whole eyes and performed HPLC analysis. We detected the Gal6S-containing oligosaccharides, (6S)GlcNAcβ1→3(6S)Galβ1→4(6S)GlcNAcβ1→3Gal and (6S)Galβ1→4(6S)GlcNAc, in KS from wild type (WT) mice (Figure 2). However, these species were not detectable in KS from $Chst1^{-/-}$ mice, indicating the loss of KSGal6ST enzymatic activity in this tissue.

KSGal6ST is selectively expressed in HEVs

Since $Chst1^{-/-}$ (hereafter, KSGal6ST KO) mice express the LacZ gene under the control of the *Chst1* promoter, we were able to use β-galactosidase activity as a surrogate for KSGal6ST expression. We performed whole-mount X-Gal

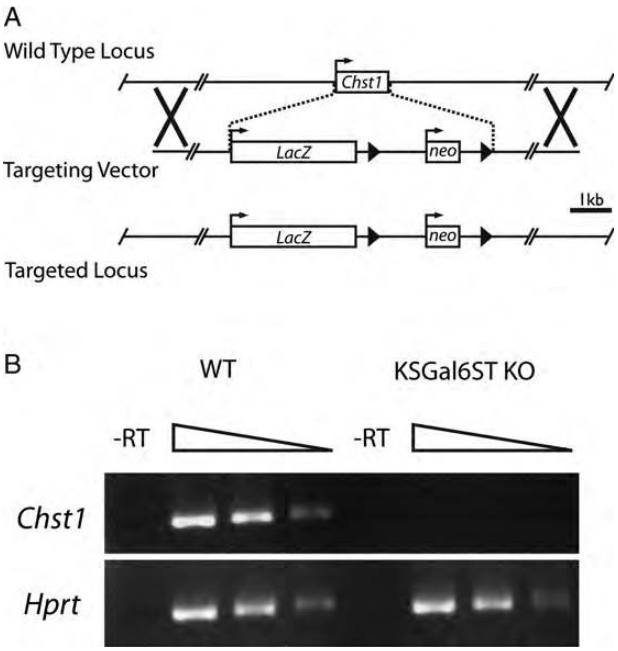

Fig. 1. Generation of KSGal6ST-deficient mice. (**A**) Schematic of the *Chst1* locus and the BAC targeting vector created by Regeneron, Inc., which replaces the entire protein-coding region of *Chst1* with the LacZ and neomycin phosphotransferase (neo) genes. Boxes represent protein-coding regions of exons. Arrows represent transcriptional start sites. Arrowheads represent loxP sites. Xs denote regions of homologous recombination. The scale bar represents 1 kb (kilobase). (**B**) PCR products generated with primers specific for *Chst1* (206 bp product) and *Hprt* (252 bp product) using 5-fold serial dilutions of cDNA from WT or KSGal6ST KO mouse cortex as a template. No products were observed when RT was omitted from the cDNA synthesis reaction. RT, reverse transcriptase; WT, wild type.

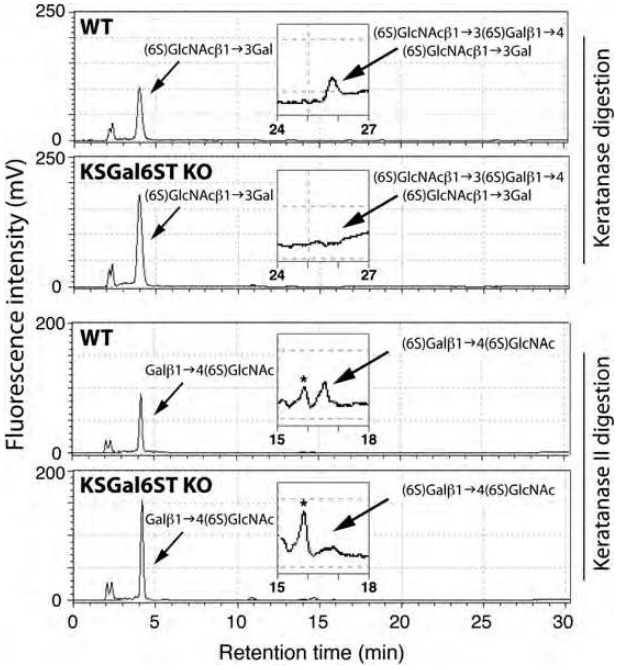

Fig. 2. KS analysis in KSGal6ST-deficient mice. Reversed-phase ion-pair chromatography analysis of ocular KS from eyes of WT and KSGal6ST KO mice. Standard substances were eluted at the peak positions indicated by arrows. Elution profiles around the peak positions of (6S)GlcNAcβ1→3(6S)Galβ1→4(6S)GlcNAcβ1→3Gal and (6S)Galβ1→4(6S)GlcNAc are magnified in insets. Peaks indicated by asterisks were not identified. WT, wild type.

staining on organs from KSGal6ST KO mice and found expression in the brain, optic nerve and eye, lung, glomeruli of the kidney and the thymus (Figure 3A). KSGal6ST expression was also present in PLN, mesenteric lymph nodes (MLN), and Peyer's patches, most prominently in branched structures resembling blood vessels (Figure 3B). Diffuse X-Gal staining was also seen in B-cell follicles in Peyer's patches. Similar staining patterns were observed in *Chst1*$^{+/-}$ animals, whereas expression was not detectable in the salivary gland, stomach, liver, heart, skeletal muscle, skin, ovary or testes from either KSGal6ST KO or *Chst1*$^{+/-}$ mice (data not shown). As expected, we did not observe X-Gal staining in any tissue from WT mice (Figure 3A).

The branched X-Gal^{+} structures in lymph nodes and Peyer's patches, coupled with the evidence that Gal6S can serve as a recognition determinant for L-selectin in vitro, prompted us to determine whether KSGal6ST was selectively expressed in HEVs. We performed immunofluorescence on tissue sections from X-Gal-stained KSGal6ST KO lymphoid organs using the endothelial cell marker CD31 and the HEV-specific antibody MECA-79, which has an absolute requirement for GlcNAc6S in the context of an extended core 1 O-glycan (Galβ1→4[6S]GlcNAcβ1→3Galβ1→3GalNAc) (Yeh et al. 2001). We found strong KSGal6ST expression in MECA-79^{+} HEVs from PLN and MLN, whereas other CD31^{+} vessels in these tissues expressed KSGal6ST only weakly (Figure 3C). In Peyer's patches, we also found selective expression of KSGal6ST in HEVs, as identified by CD31 expression and plump endothelial morphology.

KSGal6ST generates Gal6S on O-glycans in PLN

To determine whether KSGal6ST expression in lymph nodes is required to synthesize Gal6S, we performed a structural analysis of sulfated glycans in lymph nodes using MS. O-glycans were released from whole PLN extracts and permethylated, and the sulfated fractions were analyzed by MS as described previously (Khoo and Yu 2010). In WT PLN, direct matrix-assisted laser desorption/ionization (MALDI)-MS mapping in negative ion mode revealed the presence of both mono- and di-sulfated O-glycan structures, the three most abundant being the simple non-, mono- and di-*N*-glycolylneuraminic acid (Neu5Gc)-sialylated Core 2 structures. Nanoelectrospray ionization (NanoESI)-MS analysis of di-sulfated structures from WT mice showed that both sulfates were preserved to give doubly charged $[M–2H]^{2-}$ molecular ions (Figure 4A). As noted previously, the second sulfate was readily lost via MALDI in source fragmentation (Yu et al. 2009), which resulted in mono-sulfated species carrying an additional free OH group (Figure 4C). Interestingly, structures that were extended with additional LacNAc units were mostly found in the di-sulfated fraction.

To validate the identity of these sulfated O-glycan structures and to define the precise location of sulfates, the same samples were further subjected to nanoliquid chromatography (LC)-nanoESI-MS/MS analysis in negative ion mode, with each of the major components detected by MALDI-MS selected for nanoESI-HCD-MS/MS. Assignment of the sulfated residues was facilitated by diagnostic ions that were established using similar analyses of synthetic standards (Figure 4B). In WT mice, MS/MS of the mono-sulfated, mono-sialylated Core 2 structures clearly demonstrated that Gal3S, Gal6S and GlcNAc6S were present, as indicated by their diagnostic ions (Figure 4C). The ions for terminal Gal3S (*m*/*z* 153, 181) were not observed in di-sialylated Core 2 structures, consistent with this modification being precluded by α3-linked Sia on both arms. In the mono-sulfated, di-sialylated structures, only the ions derived from GlcNAc6S were detected, whereas in the di-sulfated, di-sialylated structures, additional ions at *m*/*z* 167 and 269 indicated that internal Gal6S was also present (data not shown). Likewise, in the di-sulfated mono-sialylated structures, ions indicative of internal Gal6S were found, along with the additional presence of *m*/*z* 253 and 283 derived from terminal Gal6S (Figure 4C). The paucity of 6,6′-disulfated structures suggested that terminal sialylation of LacNAc units is favored over sulfation of Gal when GlcNAc6S is present. Thus, for the most abundant sulfated O-glycans, LacNAc units on the 6-arm were most often modified with GlcNAc6S and extended to 6-sulfo-3′sLN, while sialylated Gal6S was preferentially found on the 3-arm. LacNAc units modified with GlcNAc6S could be further fucosylated, and indeed we confirmed the presence of a structure consistent with 6-sulfo-sLex by MS/MS (data not shown).

Previous biochemical analysis of GlyCAM-1 O-glycans has demonstrated that the abundance of Gal6S-containing structures is substantially increased in GlcNAc6ST1/2 DKO mice (Kawashima et al. 2005). Therefore, we chose not to analyze KSGal6ST KO mice but instead to use the GlcNAc6ST1/2 DKO background to address whether KSGal6ST was required for the generation of Gal6S-containing O-glycans in lymph

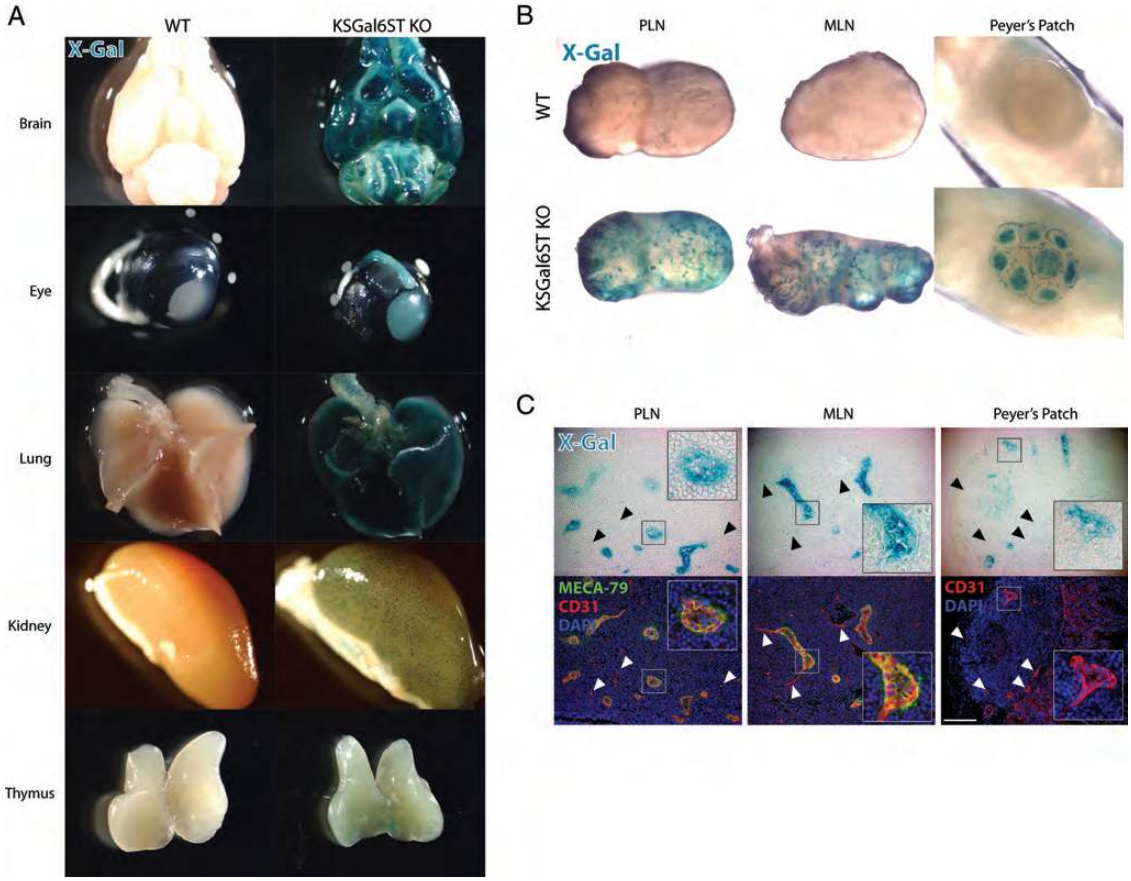

Fig. 3. KSGal6ST expression in HEVs (**A**), (**B**) Tissues from WT or KSGal6ST KO mice analyzed for β-galactosidase activity using X-Gal (blue). (**C**) Bright field images (top) of cryostat-cut sections of lymphoid organs from KSGal6ST KO mice stained with X-Gal (blue). Fluorescent images (bottom) of the same sections stained with MECA-79 (green), anti-CD31 (red) and DAPI (blue). Insets show HEVs magnified 3×. Arrowheads highlight examples of vessels with weak X-Gal staining. The scale bar represents 100 μm and applies to adjacent images. Isotype-matched control antibodies were used to establish background fluorescence. WT, wild type; PLN, peripheral lymph nodes; MLN, mesenteric lymph nodes.

nodes. We intercrossed GlcNAc6ST1/2 DKO mice (hereafter, DKO mice) with KSGal6ST KO mice to produce GlcNAc6ST-1/GlcNAc6ST-2/KSGal6ST triple KO mice (hereafter, TKO mice). These mice were born at the expected Mendelian ratio and were healthy and fertile with no gross physical or behavioral abnormalities. By MS and MS/MS analyses, as described above, we found that the MALDI-MS profile and ion intensity for the simple Core 2 O-glycans was similar between WT and DKO mice (Figure 4C). However, the diagnostic fragment ions attributed to GlcNAc6S (*m*/*z* 234, 195) were undetectable in DKO mice, while the ^{3,5}A ion at *m*/*z* 167 derived from Gal6S was the most abundant ion within the low mass region in each of the structures we examined. Thus, an increase in Gal6S in PLN from DKO mice appears to have maintained the overall amount of sulfated O-glycans, but prevented most additional LacNAc extension and fucosylation, giving rise to a much simpler MS profile. In agreement with previous biochemical analyses of GlyCAM-1 O-glycans (Kawashima et al. 2005; Hiraoka et al. 2007), 6′-sulfo-sLex was not found in WT or DKO samples. From these data, we surmise that a considerable level of 6-sulfo-3′sLN is generated in WT mice, which can then be converted to 6-sulfo-sLex, whereas additional sulfate on the 6-*O* position of Gal in 6-sulfo-LN or 6-sulfo-3′sLN is not favored. In DKO mice, this competitive inhibition may be alleviated, leading to the observed increase in Gal6S concomitant with reduced LacNAc extension along with reduced α3-linked fucose. Importantly, in PLN from TKO mice, *m*/*z* 167 derived from Gal6S was not detected in any of the structures we analyzed (Figure 4C). In fact, minimal levels of sulfated O-glycans were present, and MS/MS on the residual sulfated core 2 structures clearly showed that the remaining sulfate was a terminal Gal3S.

KSGal6ST generates sialylated, 6,6′-disulfated glycans in lymph node HEVs

As reviewed above, 6,6′-disulfo-lactose neoglycolipids are recognized by L-selectin (Bruehl et al. 2000). In addition, a previous analysis of GlyCAM-1 O-glycans was consistent with the presence of 6,6′-disulfo-sLex (Siaα2→3[6S]Galβ1→4[Fucα1→3][6S]GlcNAc) and 6,6′-disulfo-3′sLN (Siaα2→3[6S]Galβ1→4[6S]GlcNAc) in lymph nodes (Hemmerich et al. 1995). However, we were unable to detect 6,6′-disulfated structures in total lymph node O-glycans by MS. In order to

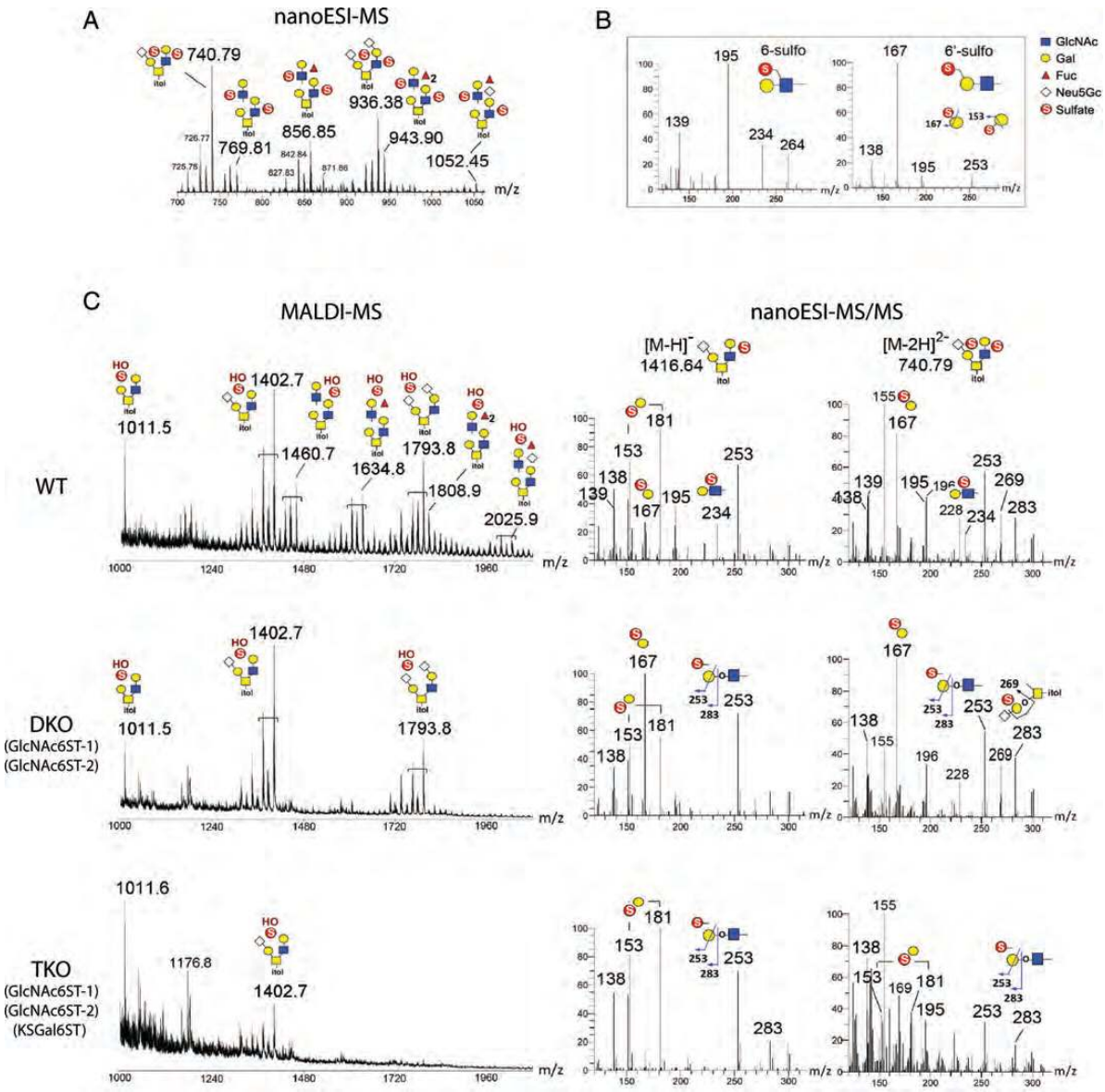

Fig. 4. MS analyses of permethylated sulfated O-glycans released from lymph nodes of KSGal6ST-deficient mice. (**A**) NanoLC-nanoESI-MS spectrum for WT di-sulfated O-glycan fractions (summed over a period of elution time for the major signals). Both sulfates were preserved under nanoESI-MS to give doubly charged $[M–2H]^{2–}$ molecular ions. (**B**) Spectra for a panel of sulfated LacNAc standards analyzed to establish the diagnostic ions produced under nanoESI-HCD MS/MS fragmentation. The singly charged low mass ions at *m/z* 195 and 234 were reproducibly detected for all internal GlcNAc6S-containing glycans. In contrast, the ^{3,5}A ion at *m/z* 167 was detected for Gal6S-containing glycans, which could be distinguished from terminal Gal3S by the ions at *m/z* 153 and 181 (not shown). (**C**) Spectra of the di-sulfated O-glycan fractions from WT, GlcNAc6ST-1/-2 DKO and GlcNAc6ST-1/-2/KSGal6ST TKO lymph nodes analyzed in negative ion mode by MALDI-MS (left). The di-sulfated O-glycans were prone to losing a sulfate by in-source fragmentation to produce $[M–H]^–$ molecular ions carrying one sulfate and one free OH group. Low mass regions of the nanoESI-HCD MS/MS spectra (right) of mono- and di-sulfated mono-sialylated core 2 structures from WT, DKO and TKO lymph nodes, annotated with diagnostic ions for sulfated structures (see B). Additional ions at *m/z* 253 (E ion) and 283 (B ion) were indicative of terminal sulfated Gal whilst *m/z* 269 (D ion) was derived from an internal sulfated Gal, as illustrated. The full spectra of each (data not shown) carried other neutral loss ions and nonreducing terminal fragment ions, which supported the assigned overall structures but did not allow differentiation of the positions of sulfates. Assignment of the major peaks for all spectra is as annotated using the standard cartoon symbols. WT, wild type; DKO, double KO; TKO, triple KO.

determine whether these structures were expressed specifically in HEVs, we took advantage of monoclonal antibodies that were generated by immunizing mice with synthetic 6,6′-disulfo-sLex glycolipids (Mitsuoka et al. 1998). We characterized the glycan specificity of these antibodies by enzyme-linked immunosorbent assay (ELISA) using a series of synthetic glycolipids coated onto plastic wells and found that G270-2 (isotype IgM) bound the 6,6′-disulfo-sLex immunogen as well as 6,6′-disulfo-3′sLN (Figure 5A). G270-2 binding exhibited an absolute requirement for Gal6S

and was reduced by ~80% in the absence of either Sia or 6-*O* sulfation of GlcNAc.

Using G270-2, we then proceeded to determine whether 6,6′-disulfo-3′sLN, or a structural analog, was present in lymphoid tissues. In PLN and MLN from WT mice, G270-2 reacted with nearly all HEVs, although the staining was unevenly distributed among endothelial cells (Figure 5B–D). In Peyer's patches, G270-2 reactivity was not observed in $CD31^+$ vessels (Figure 5E). Instead, it was present in B-cell follicles where it partially colocalized with the germinal center marker GL7 (Figure 5F). We next investigated the structural requirements for G270-2 staining. Neuraminidase treatment of tissue sections reduced G270-2 staining of HEVs to background levels (Figure 5B). Furthermore, G270-2 staining was completely absent in lymph nodes of GlcNAc6ST1/2 DKO mice (Figure 5C). Staining was also reduced to control levels in lymph nodes from KSGal6ST KO mice (Figure 5D). In contrast, we found no differences in G270-2 staining between C6ST-1 KO mice and WT mice. As expected, MECA-79 staining in HEVs was not altered in the absence of either KSGal6ST or C6ST-1. In agreement with our findings in HEVs, G270-2 staining in germinal centers was reduced to control levels by neuraminidase treatment and absent in KSGal6ST KO as well as GlcNAc6ST1/2 DKO mice (Figure 5E and F, data not shown).

KSGal6ST does not contribute to L-selectin ligand expression or lymphocyte homing

We next addressed whether the Gal6S-containing structures we detected using MS and G270-2 contribute to L-selectin ligand activity in vivo. To directly detect L-selectin ligands, we first stained lymphoid organs with an L-selectin-Fc fusion protein. HEVs were identified by their CD31 expression and plump endothelial cells. L-selectin-Fc staining of HEVs was comparable in WT and KSGal6ST KO mice (Figure 6A). Consistent with previous findings (Kawashima et al. 2005; Uchimura et al. 2005), GlcNAc6ST1/2 DKO mice showed very weak, abluminal staining of HEVs (Figure 6A). Mice deficient in L-selectin ligands exhibit a reduction in the number of lymphocytes and a decreased percentage of B cells in lymph nodes (Homeister et al. 2001; Kawashima et al. 2005; Uchimura et al. 2005; Mitoma et al. 2007; Yang et al. 2012). We observed no difference in the number of total lymphocytes in blood or lymphoid organs from KSGal6ST KO mice relative to WT mice (Figure 6B). There were small but significant decreases in B cells (3–10%) in PLN and MLN, as well as small increases in T cells (10%) in PLN, from KSGal6ST KO mice. However, these changes were also seen in the peripheral blood, consistent with systemic effects on these populations.

Since L-selectin-Fc staining and lymphoid organ cellularity may not reveal subtle defects in L-selectin ligand activity, we evaluated short-term lymphocyte homing in KSGal6ST KO mice. We injected a 1:1 mixture of WT and L-selectin KO donor splenocytes into the caudal vein of WT or KSGal6ST KO recipient mice and measured the percentage of donor cells present in lymphoid organs after 1 h. In agreement with previous findings, L-selectin KO cells were 97, 84 and 30% inhibited in their ability to home to PLN, MLN and Peyer's patches (*P* values between 0.01 and 0.0001) (Arbones et al. 1994). We did not observe any defects in the homing of WT splenocytes to lymph nodes in KSGal6ST KO mice (Figure 6C). We did find a 33% increase in the percentage of WT donor cells in Peyer's patches ($P < 0.0005$) and a 24% increase in spleens ($P < 0.05$) from KSGal6ST KO mice. However, increases in L-selectin KO donor cells were also observed. Thus, this effect does not appear to reflect changes in L-selectin-dependent homing.

Previous work has demonstrated that GlcNAc6ST1/2 DKO mice exhibit residual L-selectin-dependent homing to PLN and MLN. To address whether KSGal6ST contributes to this ligand activity, we used TKO mice deficient in KSGal6ST, as well as GlcNAc6ST-1 and GlcNAc6ST-2. Although the absence of GlcNAc6ST-1 and GlcNAc6ST-2 reduced homing by 71% in PLN ($P < 0.0001$) and 31% in MLN ($P < 0.005$), consistent with previous findings (Kawashima et al. 2005; Uchimura et al. 2005), there was no further reduction in the absence of KSGal6ST (Figure 6D). Instead, we found a 35% increase ($P < 0.005$) in L-selectin-dependent homing to PLN in TKO mice. This increase was not observed in MLN.

Discussion

Our characterization of G270-2 staining points to the presence of 6,6′-disulfo-3′sLN, or a structural analog, in lymph node HEVs. Indeed, our previous analysis of GlyCAM-1 O-glycans was consistent with the existence of this structure (Hemmerich et al. 1995). Studies using chemically synthesized glycans implicated 6,6′-disulfated structures in L-selectin recognition (Bertozzi et al. 1995; Bruehl et al. 2000). We found that G270-2 staining, though unchanged in C6ST-1 KO mice, was completely absent in KSGal6ST KO mice, providing in vivo confirmation of the Gal-6-*O*-sulfotransferase activity of KSGal6ST. Additionally, we established that KSGal6ST was required for the generation of all Gal6S-containing O-glycans that we detected by MS in GlcNAc6ST1/2 DKO PLN. Nevertheless, KSGal6ST KO mice did not exhibit a detectable deficiency in short-term lymphocyte homing. Thus, we conclude that the G270-2 epitope and the broader class of glycans generated by KSGal6ST are dispensable for L-selectin function in this setting. We were unable to confirm the absence of Gal6S on N-glycans in KSGal6ST-deficient mice, because our N-glycan profiles were not of sufficient quality. Furthermore, recombinant C6ST-1 has Gal-6-*O*-sulfotransferase activity toward desulfated corneal KS chains and, to a much lesser extent, small sialylated lactosamine structures (Habuchi et al. 1997). Thus, it is possible that C6ST-1 generates Gal6S on KS proteoglycans, N-glycans or other glycans not included in our MS analysis. However, a previous characterization of C6ST-1 KO mice found that this enzyme does not contribute to short-term homing (Uchimura et al. 2002). In addition, we generated KSGal6ST/C6ST-1 DKO mice and found no changes in homing compared with WT mice (data not shown), eliminating the possibility that C6ST-1 makes compensatory contributions to lymphocyte homing in the absence of KSGal6ST. We consider the existence of an undescribed Gal-6-*O*-sulfotransferase unlikely, given the high degree of sequence similarity among the known members of the GlcNAc-, Gal-, GalNAc-6-*O*-sulfotransferase

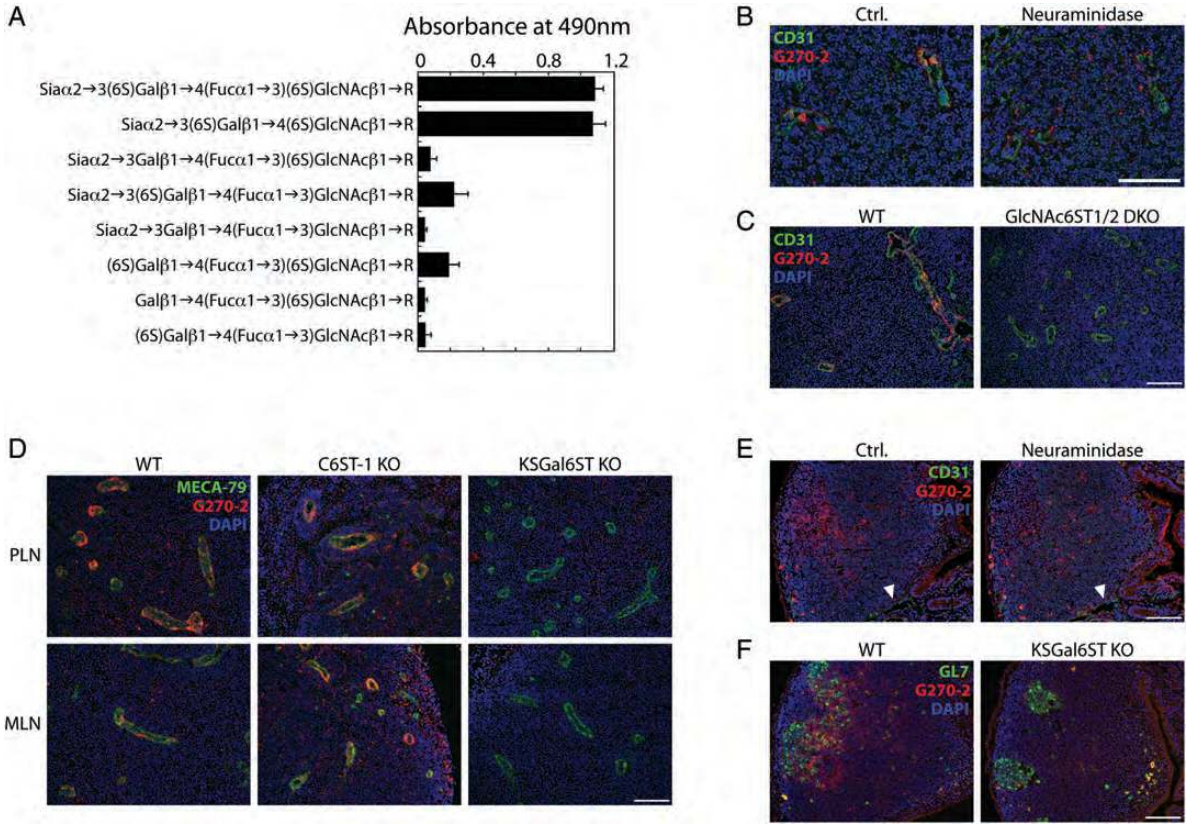

Fig. 5. Expression of sialylated 6,6′-disulfated glycans in HEVs and germinal centers of lymphoid organs. (**A**) Reactivity of G270-2 as determined by ELISA using 5 ng immobilized neoglycolipids per well. (**B**) Cryostat-cut serial sections of PLN from WT mice treated with neuraminidase or buffer alone (ctrl.), then stained with anti-CD31 (green), G270-2 (red) and DAPI (blue). (**C**) Cryostat-cut sections of PLN from WT and GlcNAc6ST-1/-2 DKO mice stained as in (**B**). (**D**) Cryostat-cut sections of PLN and MLN from WT, C6ST-1 KO and KSGal6ST KO mice stained with MECA-79 (green), G270-2 (red) and DAPI (blue). (**E**) Cryostat-cut serial sections of Peyer's patches from WT mice treated with neuraminidase or buffer alone (ctrl.), and then stained as in (**B**). Arrowheads highlight examples of $CD31^{+}$ vessels. (**F**) Cryostat-cut sections of Peyer's patches from WT and KSGal6ST KO mice stained with GL7 (green), G270-2 (red) and DAPI (blue). All scale bars represent 100 μm and apply to adjacent images. Isotype-matched control antibodies were used to establish background fluorescence. PLN, peripheral lymph nodes; MLN, mesenteric lymph nodes; WT, wild type; DKO, double KO.

subfamily of sulfotransferases (Fukuda et al. 2001). Thus, we conclude that Gal6S does not contribute to L-selectin ligand activity during normal lymphocyte homing.

We also show that KSGal6ST does not contribute to the residual lymphocyte homing in GlcNAc6ST1/2 DKO mice. A previous analysis of GlyCAM-1 O-glycans revealed small amounts of GlcNAc6S on core 2 glycans in DKO mice (Kawashima et al. 2005), which could be responsible for the residual homing in both DKO and TKO mice. Our MS analysis is consistent with this result, since we detected low levels of 6-sulfo-3′sLN on core 2 glycans in PLN of TKO mice. GlcNAc6ST-4 (*Chst7*) may be involved in generating these structures, since it is expressed in HEVs (Kawashima et al. 2005). However, we and others have recently shown that injection of an antibody that recognizes 6-sulfo-sLex on both O- and N-glycans fails to reduce residual homing to lymph nodes in DKO mice, indicating that the low level of 6-sulfo-sLex does not account for the residual ligand activity (Hirakawa et al. 2010; Arata-Kawai et al. 2011). The remaining ligands are likely to involve structures related to sLex, since injection of soluble E-selectin, which binds to sLex, blocks the residual lymphocyte homing to DKO PLN (Uchimura et al. 2005). Furthermore, sLex is sufficient for L-selectin-Fc binding (Foxall et al. 1992) and is surmised to be sufficient for L-selectin-dependent rolling on endothelial ligands in vitro (Tangemann et al. 1999; Li et al. 2001). Based on these observations, the simplest explanation for the residual lymphocyte homing to PLN in DKO and TKO mice is that it involves suboptimal binding of L-selectin to structures that terminate in sLex lacking sulfation, as previously proposed (Kawashima et al. 2005).

Although the functions of Gal6S in HEVs are still unclear, we show that L-selectin-dependent homing to PLN is increased by 35% in TKO mice relative to DKO mice. These data are consistent with the possibility that this sulfate modification negatively regulates lymphocyte homing in some circumstances. Recombinant FucT-IV and FucT-VII cannot act on 6′-sulfo-3′sLN (Homeister et al. 2001), and recombinant KSGal6ST cannot act on sLex (Torii et al. 2000). Consistent with these findings, 6′-sulfo-sLex was not detected in HPLC analyses of GlyCAM-1 O-glycans (Kawashima et al. 2005; Hiraoka et al. 2007) or in the present MS analysis of total

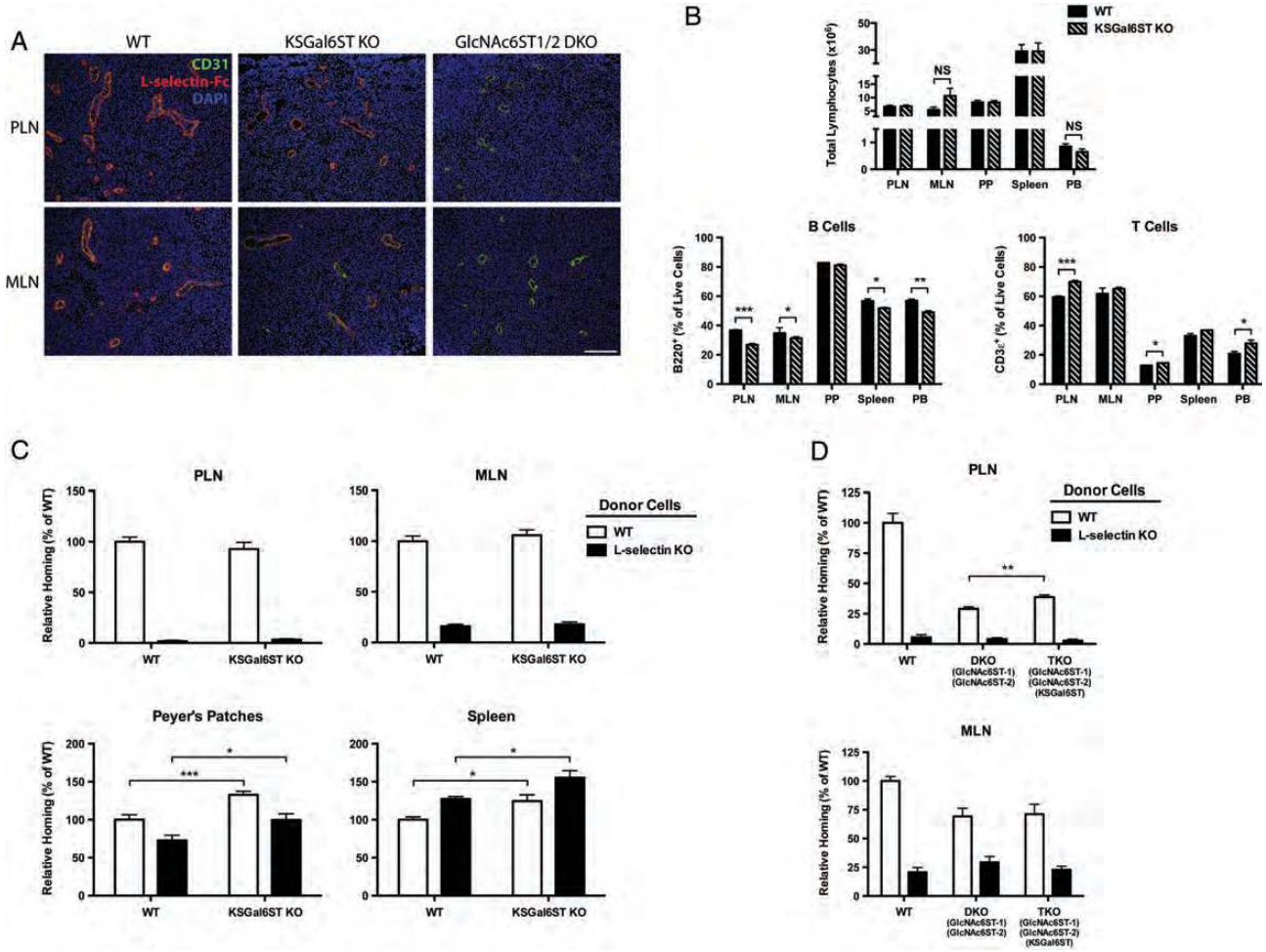

Fig. 6. L-selectin ligand expression, lymphocyte numbers and lymphocyte homing in KSGal6ST-deficient mice. (**A**) Cryostat-cut sections of PLN and MLN from WT, KSGal6ST KO and GlcNAc6ST-1/-2 DKO mice stained with anti-CD31 (green), L-selectin-Fc (red) and DAPI (blue). Background fluorescence was established by staining separate sections with L-selectin-Fc in the presence of 10 mM EDTA. The scale bar represents 100 μm and applies to adjacent images. (**B**) Total numbers (top) and percentages (bottom) of $CD3\varepsilon^+$ T cells and $B220^+$ B cells in peripheral blood and lymphoid organs from WT ($n = 4$) and KSGal6ST KO ($n = 3$) mice. For MLN, $n = 5$ for WT, and $n = 6$ for KSGal6ST KO ($P = 0.14$). (**C**) Short-term lymphocyte homing to PLN, MLN, Peyer's patches and spleens of WT ($n = 11$) and KSGal6ST KO ($n = 15$) mice. Pooled results from three independent experiments are shown. (**D**) Short-term homing of splenocytes to PLN and MLN of WT ($n = 6$), GlcNAc6ST-1/-2 DKO ($n = 7$) and GlcNAc6ST-1/-2/KSGal6ST TKO ($n = 8$) mice. Pooled results from two independent experiments are shown. Differences between mouse genotypes are not significant unless otherwise noted. Homing of L-selectin KO splenocytes was significantly reduced relative to WT splenocytes in all cases, except in homing to the spleen, where it was significantly enhanced (P values between 0.01 and 0.0001). Homing of WT splenocytes to PLN ($P < 0.0001$) and MLN ($P < 0.005$) was significantly reduced in DKO recipients relative to WT recipients. PLN, peripheral lymph nodes; MLN, mesenteric lymph nodes; PP, Peyer's patches; SPLN, spleen; PB, peripheral blood; WT, wild type; DKO, double KO; TKO, triple KO; NS, not significant; $*P < 0.05$; $**P < 0.005$; $***P < 0.0005$.

PLN O-glycans. Furthermore, CHO cell monolayers stably expressing CD34, FucT-VII and GlcNAc6ST-1 have a reduced capacity to support lymphocyte rolling upon transient overexpression of KSGal6ST (Hiraoka et al. 2007). Thus, it has been proposed that the addition of sulfate to the 6-*O* position of Gal precludes the generation of L-selectin ligands by inhibiting the addition of α3 linked fucose on GlcNAc (Hiraoka et al. 2007). Since sLex is plausibly responsible for the residual homing in DKO mice, as discussed above, KSGal6ST deficiency may enhance this residual homing by allowing increased generation of sLex structures. Future studies examining the levels of sLex in TKO mice should address this hypothesis.

In contrast to our observations comparing DKO mice with TKO mice, we did not find that the absence of KSGal6ST alone enhances L-selectin-dependent homing. Multiple factors could account for this discrepancy. First, Gal6S appears to be less abundant in WT PLN than in DKO PLN, as suggested by a previous analysis of GlyCAM-1 O-glycans (Kawashima et al. 2005) and our current MS analysis of PLN O-glycans. This effect is likely due to the increased availability of the sulfate donor PAPS in DKO mice, as previously proposed (Kawashima et al. 2005). The low abundance of Gal6S in WT HEVs may result in a negligible increase in sLex structures in KSGal6ST KO mice and, hence, insignificant effects on homing. A second possibility is that 6-sulfo-sLex in WT HEVs makes the predominant contribution to L-selectin ligand activity such that additional sLex generated in the absence of Gal6S does not appreciably increase homing.

Regardless of the mechanisms underlying these differential effects of Gal6S on homing, it will be important to determine whether KSGal6ST influences leukocyte trafficking in other settings. For example, HEVs can develop during many chronic inflammatory diseases including rheumatoid arthritis, psoriasis and ulcerative colitis (Drayton et al. 2006). Moreover, HEV-like vessels are induced in mouse models of chronic inflammation and tertiary lymphoid organ formation. The LacZ reporter allele and the monoclonal antibody G270-2 described in this report provide tools for determining whether KSGal6ST and 6,6′-disulfo-sLN are expressed in the HEV-like vessels at these ectopic lymphoid sites.

Our survey of KSGal6ST expression highlights several other tissues where Gal6S could have important functions. The intensity of X-Gal staining was strongest in the brain, which is in agreement with previously observed transcript levels in mice and humans. It has been shown that GlcNAc6ST-1 is required for 6-*O* sulfation of GlcNAc on KS in the mouse central nervous system (Zhang et al. 2006). Furthermore, these studies demonstrated that GlcNAc6ST-1 deficiency impairs glial scar formation and enhances neurite outgrowth after traumatic injury. Experiments using KSGal6ST KO mice can address similar questions with respect to Gal6S in the brain. KS is also critical for normal corneal morphology and function, as evidenced by humans with mutations in the GlcNAc-6-*O*-sulfotransferase gene *CHST6* (c-GlcNAc6ST) (Akama et al. 2000), and mice with a targeted deletion in *Chst5* (i-GlcNAc6ST) (Hayashida et al. 2006). Furthermore, the monoclonal antibody 5D4, which recognizes a Gal6S-containing epitope within KS (Mehmet et al. 1986), stains the cornea (Hayashida et al. 2006) and retina (Ng and Streilein 2001). Although we were unable to detect KSGal6ST expression in the cornea, we did detect strong expression in the retina and optic nerve. Our HPLC analysis establishes that KSGal6ST is required for generating Gal6S within ocular KS. Thus, KSGal6ST KO mice will be useful in determining whether this modification contributes to KS function in the eye.

We found KSGal6ST expression in the glomeruli of the kidney. The core protein of the KS proteoglycan lumican is expressed in the glomerular endothelial cell coat (Friden et al. 2011). Therefore, KSGal6ST may participate in sulfating KS chains on this proteoglycan scaffold. Additionally, the cell-surface mucin podocalyxin is expressed in foot processes of podocytes in the glomeruli (Nielsen and McNagny 2009). Podocalyxin is required for the formation of the slit diaphragms through which blood plasma is filtered before entering the urinary space. The negative charge of podocalyxin, imparted by its sulfation and sialylation, is thought to be important for its function (Dekan et al. 1991). Accordingly, mice with a mutation in the Sia biosynthesis enzyme, GNE, do not form slit diaphragms and die from renal failure soon after birth (Galeano et al. 2007). Although we observed no gross morphological differences in glomeruli from KSGal6ST KO mice, it remains to be determined whether KSGal6ST contributes to the sulfation of podocalyxin and affects its function in glomerular filtration.

We also found KSGal6ST expression as well as G270-2 reactivity in germinal centers of Peyer's patches and MLN. This staining has the same structural requirements as in HEVs and thus indicates the presence of 6,6′-disulfo-3′sLN, or a structural analog. B cells express CD22, a member of the Siglec family that is known to negatively regulate B cell activation (Walker and Smith 2008). Sia on the 6-*O* position of Gal is required for CD22 binding (Paulson et al. 2012). Therefore, it is plausible that KSGal6ST impedes the generation of CD22 ligands by competing with α6 sialyltransferases. It will be of interest to examine KSGal6ST KO mice in this context.

Sulfate serves as a recognition determinant for many immunological receptors. These include C-type lectins such as L-selectin, P-selectin and the macrophage mannose receptor, as well as Siglecs such as Siglec-7, Siglec-9 and CD22 (Campanero-Rhodes et al. 2006; Kimura et al. 2007; Miyazaki et al. 2012). Screening of lectins using the consortium for functional glycomics (CFG) glycan array has suggested the importance of Gal6S in ligands for several receptors on innate immune cells. Siglec-8, a Sia-binding lectin expressed on human eosinophils, binds 6′sulfo-sLex and 6′sulfo-3′sLN with remarkable specificity and shows an absolute requirement for sulfate on the 6-*O* position of Gal (Bochner et al. 2005). Human Siglec-7 and Siglec-5 and murine Siglec-E and Siglec-F bind 6′sulfo-sLex, but also show binding to glycans lacking Gal6S (Tateno et al. 2005). The C-type lectin, langerin preferentially binds to 6′-sulfo-lactosamine on the glycan array, and also binds CHO cells transfected with KSGal6ST (Tateno et al. 2010). Notably, we found strong KSGal6ST expression in the lung, where it could potentially generate structures recognized by resident dendritic cells, which express langerin. KSGal6ST KO mice should provide a valuable tool for determining whether these receptors recognize Gal6S-containing structures in vivo.

Materials and methods

Mice

Chst1$^{-/-}$ mice were generated by Regeneron Pharmaceuticals, Inc. and the trans-NIH Knockout Mouse Project (KOMP) using published protocols (Valenzuela et al. 2003). Detailed information about the targeting construct is available on the Velocigene website (http://www.velocigene.com/komp/detail/10172). Briefly, upon recombination with the bacterial artificial chromosome targeting vector, a cassette containing the promoterless *Escherichia coli* K12 LacZ gene and the neomycin phosphotransferase gene was introduced in place of the entire protein-coding region of *Chst1*. C57BL/6NTac embryonic stem cells were screened for the loss of one WT copy of *Chst1* using Taqman quantitative PCR. Targeted embryonic stem cells were injected into BALB/c blastocysts, and the resulting chimeric offspring were bred until germline transmission was achieved. Mice deficient in GlcNAc6ST-1, GlcNAc6ST-2 and L-selectin have been described previously (Arbones et al. 1994; Uchimura et al. 2005). L-selectin KO mice were genotyped by fluorescence-assisted cell sorting (FACS) analysis of peripheral blood leukocytes stained with fluorescein isothiocyanate (FITC)-anti-mouse L-selectin (clone MEL-14, eBioscience). Sulfotransferase-deficient mice were genotyped by PCR as previously described (Uchimura et al. 2005). Primers specific for the genes *Chst1* (5′-CCTCTG CAACCACAACTCTC-3′, 5′-GCCTTCCAAGAACATTGCA T-3′), *Chst2* (5′-AAGCCTACAGGTGGTGCGAA-3′, 5′-CA GGACTGTTAACCCGCTCA-3′), *Chst3* (5′-ATGCATCTCTC

TTGTCCCTGA-3′, 5′-CACATACAGGTCGCATAGCAA-3′), *Chst4* (5′-GTAGCTCTCTTCATCCATATGTTCG-3′, 5′-CGTTTCCAAATGCTGCCCTAGCAC-3′) and LacZ (5′-GTCTGTCCTAGCTTCCTCACTG-3′) were obtained from IDT. Alternate primers were use to detect the *Chst2*$^{-/-}$ allele (5′-GCCAAAAGTGATCACCTCGT-3′), *Chst3*$^{-/-}$ allele (5′-AGGGCTATGTCTCACTGCCA-3′) and *Chst4*$^{-/-}$ allele (5′-GGCTGTGCTGCTGGTGAAAGTCAT-3′) in combination with a primer specific for the neomycin phosphotransferase gene (5′-AGCGTTGGCTACCCGTGATA-3′). C57BL/6J mice were obtained from Jackson Laboratories. All procedures involving animals were approved by the University California San Francisco Institutional Animal Care and Use Committee, and carried out in accordance with the guidelines established by the National Institutes of Health.

Reverse transcriptase PCR

The mouse forebrain was homogenized by sonication in RLT buffer (Qiagen). A total RNA was extracted using RNeasy mini kit (Qiagen) according to manufacturer's instructions. cDNA was synthesized using superscript III RT (Invitrogen) according to the manufacturer's instructions. PCR was performed as above using primers specific for *Chst1* (5′-TTGGCAGCCGAGGCTTGTCG-3′, 5′-TGCCGTACCAAAGCCGCCAG-3′) and *Hprt* (5′-TTGCTGGTGAAAAGGACCTCTCG-3′, 5′-CCACAGGACTAGAACACCTGCTAA-3′).

Preparation and structural analysis of ocular KS

Ocular KS was isolated and analyzed as described previously for heparan sulfate (Hosono-Fukao et al. 2011) with slight modifications. Adult mouse eyes (∼50 mg) were suspended in 2 mL of 0.2 N NaOH and incubated at room temperature overnight. The samples were neutralized with 4 N HCl and then treated with DNase I and RNase A (0.04 mg/mL each) (Roche) in 50 mM Tris–HCl, pH 8.0, 10 mM $MgCl_2$ for 3 h at 37°C, followed by treatment with actinase E (0.08 mg/mL) (Kaken Pharmaceutical Co., Ltd., Tokyo, Japan) at 50°C overnight. Samples were heated to inactivate enzymes, centrifuged at 5000 × *g* and 4°C for 10 min, and the supernatant was collected and mixed with an equal volume of 50 mM Tris–HCl, pH 7.2. KS was purified by diethylaminoethanol (DEAE)-Sepharose column chromatography. The oligosaccharide compositions of KS after digestion with keratanase or keratanase II overnight were determined by reversed-phase ion-pair chromatography with post-column fluorescent labeling. Gal6S-containing oligosaccharide components were identified using authentic sulfated oligosaccharide markers and digestion products released from bovine corneal KS by the action of *endo*-β-galactosidase or keratanase. KS from bovine cornea, *endo*-β-galactosidase (*Escherichia freundii*), keratanase (*Pseudomonas* sp.) and keratanase II (*Bacillus* sp. Ks 36) were purchased from Seikagaku, Tokyo, Japan.

X-Gal and immunofluorescence staining

For X-Gal staining, tissues were fixed, washed and stained with X-Gal staining solutions (Millipore) according to manufacturer's instructions, with incubation in X-Gal overnight. Tissues not stained with X-Gal were fixed in 4% PFA for 1 h, then incubated in 30% sucrose overnight. All tissues were embedded in OCT compound (Sakura Finetek) and frozen by immersion in 2-methylbutane chilled in liquid nitrogen. Tissues were sectioned at 5 μm thickness in a cryostat and then fixed in −20°C acetone for 10 min. For neuraminidase experiments, sections were treated with 50 mU/mL *Arthrobacter ureafaciens* neuraminidase (Roche Applied Sciences) in pH 5.0 acetate buffer at 37°C for 1 h. Sections were blocked with 3% bovine serum albumin (BSA) and 5% normal sera from mouse, rat, goat or donkey (Sigma), depending on the experiment. MECA-79 (BioLegend), biotin-MECA-79 (BioLegend), CD31 (Goat pAb, R&D Systems), biotin-CD31 (clone 390, eBioscience), human L-selectin-IgG (R&D Systems) and GL7 (eBioscience) were incubated with sections at 1–5 μg/mL for 1 h. G270-2 was incubated with sections at 10 μg/mL for 6 h. Nonspecific rat IgM (clone eBRM, eBioscience), biotin-rat IgM (clone eBRM, eBioscience), mouse IgM (clone 11E10, eBioscience) and goat IgG (Invitrogen) were used to establish background fluorescence. For L-selectin-Fc staining, background fluorescence was established using control sections stained in the presence of 10 mM ethylenediaminetetraacetic acid (EDTA). Secondary reagents, indocarbocyanine (Cy3)-goat anti-rat IgM, cyanine (Cy2)-goat anti-rat IgG, Cy2-streptavidin and Cy3-streptavidin were obtained from Jackson ImmunoResearch and incubated with sections at 1 μg/mL for 30 min. All antibodies were diluted in Dulbecco's phosphate buffered saline (PBS) with 3% BSA. All sections were incubated with DAPI (Invitrogen) at 0.5 μg/mL in PBS for 5 min to label nuclei. Images were acquired using a Nikon Optiphot microscope equipped with an AxioCam HR at fixed exposure. Multichannel images were created and processed in parallel using Photoshop software (Adobe).

MS analysis

O-glycan samples were prepared from whole PLN lysates, permethylated and fractionated into non-, mono- and di-sulfated fractions for MALDI-MS analyses as described previously (Yu et al. 2009; Khoo and Yu 2010). NanoLC-MS/MS analyses of the permethylated sulfated glycans were performed on a nanoACQUITY UPLC System (Waters) coupled to an LTQ-Orbitrap Velos hybrid mass spectrometer (Thermo Scientific) using the same nanoLC conditions and MS acquisition method as described previously (Shibata et al. 2012). NanoLC-MS/MS of the disulfated glycans was additionally carried out on a homemade nanoLC system comprised of a 50 μm × 4 cm homemade polystyrene-divinylbenzene (PS-DVB) monolithic trap column and a 20 μm × 4 m homemade PS-DVB grafted open tubular analytical column coupled to the same LTQ-Orbitrap Velos MS system. For this nanoLC system, sample was dissolved in 25% acetonitrile and separated at a constant flow rate of 150 nL/min, with a linear gradient of 10–40% acetonitrile (with 1 mM ammonium bicarbonate) over the course of 30 min, then increased to 80% acetonitrile over the course of 5 min and held isocratically for another 10 min. The eluent was interfaced to the nanospray source based on the liquid junction configuration consisting of an uncoated emitter and a high-voltage electrode. For each

data-dependent acquisition cycle, the full-scan MS spectrum (m/z 500–2000) was acquired in the Orbitrap at 60,000 resolution (at m/z 400) with automatic gain control (AGC) target value of 5×10^6. A target precursor inclusion list was applied to precede further selection of five most intense ions with intensity threshold of 300 counts for both collision-induced dissociation (CID) and higher energy C-trap dissociation (HCD). The AGC target value and normalized collision energy applied for CID and HCD experiments were set as 20,000, 45% and 100,000, 100%, respectively. All MS/MS data were interpreted manually.

Generation of the monoclonal antibody G270-2

G270-2 was generated as described previously (Mitsuoka et al. 1998). Briefly, 6,6′-disulfo-sLex glycolipids were adsorbed to *Salmonella minnesota* strain R595 and administered to Balb/c mice by repeated intraperitoneal injection. Splenocytes were harvested and fused with the mouse myeloma P3/X63-Ag8U1, and clones were screened for reactivity to the immunogen. The specificity of G270-2 was determined by ELISA using immobilized glycolipids as described previously (Mitsuoka et al. 1998).

Lymphocyte homing assay

Short-term lymphocyte homing assays were carried out as described previously (Arbones et al. 1994), with slight modifications. Briefly, spleens from 10- to 12-week-old C57BL/6 WT or L-selectin KO mice were mechanically dissociated with a syringe plunger and a 70 μm cell strainer (BD Biosciences). Erythrocytes were lysed using ammonium chloride buffer (150 mM NH_4Cl, 10 mM $KHCO_3$, 100 μM EDTA). Splenocytes of one genotype were incubated with 2 μM carboxyfluorescein diacetate-succinimidyl ester (CFDA-SE) (Invitrogen), while splenocytes of the other genotype were incubated with 1 μM chloromethyl tetramethylrhodamine (CMTMR) (Invitrogen), for 25 min in RPMI-1640 medium containing 0.2% FBS. Differentially labeled WT and L-selectin KO splenocytes were washed with RPMI-1640 containing 2% FBS and combined in equal numbers. A 200 μL aliquot containing 20×10^6 total cells was injected into the lateral caudal vein of each age-matched (8–10 week old), sex-matched WT, KSGal6ST KO, GlcNAc6ST1/2 DKO or TKO mouse. After 1 h, inguinal, axillary and brachial lymph nodes, all mesenteric lymph nodes, all Peyer's patches and spleens were collected. Lymph nodes were dispersed using ground glass microscope slides. Peyer's patches and spleens were mechanically dispersed using cell strainers, as above. Splenic erythrocytes were lysed using ammonium chloride buffer. All cell suspensions were filtered through 100 μm nylon mesh (ELKO Filtering Co, Miami, FL), and analyzed using a BD FACSort cytometer equipped with the CellQuest software (BD). Further analysis was carried out using the FlowJo software (Treestar Inc, Ashland, OR). The frequencies of WT and KO donor splenocytes relative to recipient cells in lymphoid organs were determined and normalized using the ratio of WT to KO cells injected, as determined by FACS analysis.

Flow cytometry analysis of blood and lymphoid organs

Blood (200 μL) was collected through the right ventricle into 5 mM EDTA, and then treated with ammonium chloride buffer to lyse erythrocytes. Lymphoid organs were collected and dissociated as described above. Cell numbers were determined using CountBright counting beads (Invitrogen) according to the manufacturer's instructions. Separate aliquots of cells were incubated with 10 μg/mL anti-mouse CD16/32 (clone 93, eBioscience) and then stained with 5 μg/mL FITC-anti-mouse CD3ε (clone 145-2C11, BioLegend) and allophycocumarin (APC)-anti-mouse B220 (clone RA3-6B2, BioLegend). Viability was determined by adding 50 μL/mL of 7-animo-actinomycin D (7AAD) solution (BD Pharmingen). Cells were analyzed using the instrumentation and software described above.

Statistical analysis

All graphical data were plotted as means plus the standard error mean, using Prism 5 software (GraphPad Software, La Jolla, CA). Student's t-test was used to establish statistically significant differences between groups.

Funding

This work was supported by the National Institutes of Health [GM-23547, GM-57411 to S.D.R., U01HG004085 to Velocigene at Regeneron, Inc., U01HG004080 to the CSD Consortium, U42RR024244 to the KOMP Repository at University of California, Davis]; the Academia Sinica and Taiwan National Science Council [grant number 99-2311-B-001-021-MY3 to K.-H.K.]; the Ministry of Education, Culture, Sports, Science and Technology [Grant-in-Aid 24590364 to R.K.]; the Ministry of Health and Welfare [Grant-in-Aid for the Third-Term Comprehensive Ten-Year Strategy for Cancer Control to R.K.]; and the Taiwan National Core Facility Program for Biotechnology [NSC100-2325-B-001-029, NSC101-2319-B-001-003 to the Core Facilities for Protein Structural Analysis at Academia Sinica].

Acknowledgements

We are grateful to Y.-Q. Wang, M. Elin and M. Izawa for technical assistance. Additional technical support with nanoLC-MS/MS data acquisition was provided by Dr. Chi-Chi Chou.

Conflict of interest

None declared.

Abbreviations

7AAD, 7-animo-actinomycin D; AGC, automatic gain control; APC, allophycocumarin; BSA, bovine serum albumin; C6ST-1, chondroitin 6-*O*-sulfotransferase-1; CFDA-SE, carboxyfluorescein diacetate succinimidyl ester; CFG, consortium for functional glycomics; CHO, Chinese hamster ovary; CID, collision-induced dissociation; CMTMR, chloromethyl tetramethylrhodamine; Cy2, cyanine; Cy3, indocarbocyanine; DEAE, diethylaminoethanol; EDTA, ethylenediaminetetraacetic acid; ELISA, enzyme-linked immunosorbent assay; ESI,

electrospray ionization; FACS, fluorescence-assisted cell sorting; FBS, fetal bovine serum; FITC, fluorescein isothiocyanate; Fuc, fucose; Gal, galactose; Gal6S, galactose-6-*O*-sulfate; GalNAc, *N*-acetylgalactosamine; Glc, glucose; GlcNAc, *N*-acetylglucosamine; GlcNAc6S, *N*-acetylglucosamine-6-*O*-sulfate; HCD, higher energy C-trap dissociation; HEVs, high endothelial venules; HPLC, high-performance liquid chromatography; HSPGs, Heparan sulfate proteoglycans; KS, keratan sulfate; KSGal6ST, keratan sulfate galactose 6-*O*-sulfotransferase; LacNAc, *N*-acetyllactosamine; LC, liquid chromatography; MALDI, matrix-assisted laser desorption/ionization; MLN, mesenteric lymph nodes; MS, mass spectrometry; Neu5Gc, *N*-glycolylneuraminic acid; OCT, optimal cutting temperature; PBS, Dulbecco's phosphate buffered saline; PCR, polymerase chain reaction; PFA, paraformaldehyde; PLN, peripheral lymph nodes; PS-DVB, polystyrene-divinylbenzene; RT, reverse transcriptase; Sia, sialic acid; TKO, triple knockout mice; WT, wild type.

References

Akama TO, Nishida K, Nakayama J, Watanabe H, Ozaki K, Nakamura T, Dota A, Kawasaki S, Inoue Y, Maeda N, et al. 2000. Macular corneal dystrophy type I and type II are caused by distinct mutations in a new sulphotransferase gene. *Nat Genet*. 26:237–241.

Arata-Kawai H, Singer MS, Bistrup A, Zante A, Wang YQ, Ito Y, Bao X, Hemmerich S, Fukuda M, Rosen SD. 2011. Functional contributions of N- and O-glycans to L-selectin ligands in murine and human lymphoid organs. *Am J Pathol*. 178:423–433.

Arbones ML, Ord DC, Ley K, Ratech H, Maynard-Curry C, Otten G, Capon DJ, Tedder TF. 1994. Lymphocyte homing and leukocyte rolling and migration are impaired in L-selectin-deficient mice. *Immunity.* 1: 247–260.

Baenziger JU. 2003. Glycoprotein hormone GalNAc-4-sulphotransferase. *Biochem Soc Trans*. 31:326–330.

Bertozzi CR, Fukuda S, Rosen SD. 1995. Sulfated disaccharide inhibitors of L-selectin: Deriving structural leads from a physiological selectin ligand. *Biochemistry.* 34:14271–14278.

Bhavanandan VP, Meyer K. 1967. Studies on keratosulfates. Methylation and partial acid hydrolysis of bovine corneal keratosulfate. *J Biol Chem*. 242:4352–4359.

Bishop JR, Schuksz M, Esko JD. 2007. Heparan sulphate proteoglycans fine-tune mammalian physiology. *Nature*. 446:1030–1037.

Bistrup A, Bhakta S, Lee JK, Belov YY, Gunn MD, Zuo FR, Huang CC, Kannagi R, Rosen SD, Hemmerich S. 1999. Sulfotransferases of two specificities function in the reconstitution of high endothelial cell ligands for L-selectin. *J Cell Biol*. 145:899–910.

Bochner BS, Alvarez RA, Mehta P, Bovin NV, Blixt O, White JR, Schnaar RL. 2005. Glycan array screening reveals a candidate ligand for Siglec-8. *J Biol Chem*. 280:4307–4312.

Borghei A, Ouyang YB, Westmuckett AD, Marcello MR, Landel CP, Evans JP, Moore KL. 2006. Targeted disruption of tyrosylprotein sulfotransferase-2, an enzyme that catalyzes post-translational protein tyrosine O-sulfation, causes male infertility. *J Biol Chem*. 281:9423–9431.

Bruehl RE, Bertozzi CR, Rosen SD. 2000. Minimal sulfated carbohydrates for recognition by L-selectin and the MECA-79 antibody. *J Biol Chem*. 275:32642–32648.

Bulow HE, Hobert O. 2006. The molecular diversity of glycosaminoglycans shapes animal development. *Annu Rev Cell Dev Biol*. 22:375–407.

Butcher EC, Picker LJ. 1996. Lymphocyte homing and homeostasis. *Science*. 272:60–66.

Campanero-Rhodes MA, Childs RA, Kiso M, Komba S, Le Narvor C, Warren J, Otto D, Crocker PR, Feizi T. 2006. Carbohydrate microarrays reveal sulphation as a modulator of siglec binding. *Biochem Biophys Res Commun*. 344:1141–1146.

Dekan G, Gabel C, Farquhar MG. 1991. Sulfate contributes to the negative charge of podocalyxin, the major sialoglycoprotein of the glomerular filtration slits. *Proc Natl Acad Sci USA*. 88:5398–5402.

Drayton DL, Liao S, Mounzer RH, Ruddle NH. 2006. Lymphoid organ development: From ontogeny to neogenesis. *Nat Immunol*. 7:344–353.

Foxall C, Watson SR, Dowbenko D, Fennie C, Lasky LA, Kiso M, Hasegawa A, Asa D, Brandley BK. 1992. The three members of the selectin receptor family recognize a common carbohydrate epitope, the sialyl Lewis(x) oligosaccharide. *J Cell Biol*. 117:895–902.

Friden V, Oveland E, Tenstad O, Ebefors K, Nystrom J, Nilsson UA, Haraldsson B. 2011. The glomerular endothelial cell coat is essential for glomerular filtration. *Kidney Int*. 79:1322–1330.

Fukuda M, Hiraoka N, Akama TO, Fukuda MN. 2001. Carbohydrate-modifying sulfotransferases: Structure, function, and pathophysiology. *J Biol Chem*. 276:47747–47750.

Fukuta M, Inazawa J, Torii T, Tsuzuki K, Shimada E, Habuchi O. 1997. Molecular cloning and characterization of human keratan sulfate Gal-6-sulfotransferase. *J Biol Chem*. 272:32321–32328.

Galeano B, Klootwijk R, Manoli I, Sun M, Ciccone C, Darvish D, Starost MF, Zerfas PM, Hoffmann VJ, Hoogstraten-Miller S, et al. 2007. Mutation in the key enzyme of sialic acid biosynthesis causes severe glomerular proteinuria and is rescued by *N*-acetylmannosamine. *J Clin Invest*. 117:1585–1594.

Galustian C, Lawson AM, Komba S, Ishida H, Kiso M, Feizi T. 1997. Sialyl-Lewis(x) sequence 6-*O*-sulfated at *N*-acetylglucosamine rather than at galactose is the preferred ligand for L-selectin and de-N-acetylation of the sialic acid enhances the binding strength. *Biochem Biophys Res Commun*. 240:748–751.

Grunwell JR, Bertozzi CR. 2002. Carbohydrate sulfotransferases of the GalNAc/Gal/GlcNAc6ST family. *Biochemistry.* 41:13117–13126.

Habuchi O, Hirahara Y, Uchimura K, Fukuta M. 1996. Enzymatic sulfation of galactose residue of keratan sulfate by chondroitin 6-sulfotransferase. *Glycobiology.* 6:51–57.

Habuchi O, Suzuki Y, Fukuta M. 1997. Sulfation of sialyl lactosamine oligosaccharides by chondroitin 6-sulfotransferase. *Glycobiology.* 7:405–412.

Hayashida Y, Akama TO, Beecher N, Lewis P, Young RD, Meek KM, Kerr B, Hughes CE, Caterson B, Tanigami A, et al. 2006. Matrix morphogenesis in cornea is mediated by the modification of keratan sulfate by GlcNAc 6-*O*-sulfotransferase. *Proc Natl Acad Sci USA*. 103:13333–13338.

Hemmerich S, Bertozzi CR, Leffler H, Rosen SD. 1994. Identification of the sulfated monosaccharides of GlyCAM-1, an endothelial-derived ligand for L-selectin. *Biochemistry.* 33:4820–4829.

Hemmerich S, Leffler H, Rosen SD. 1995. Structure of the O-glycans in GlyCAM-1, an endothelial-derived ligand for L-selectin. *J Biol Chem*. 270:12035–12047.

Hernandez Mir G, Helin J, Skarp KP, Cummings RD, Makitie A, Renkonen R, Leppanen A. 2009. Glycoforms of human endothelial CD34 that bind L-selectin carry sulfated sialyl Lewis x capped O- and N-glycans. *Blood*. 114:733–741.

Hirakawa J, Tsuboi K, Sato K, Kobayashi M, Watanabe S, Takakura A, Imai Y, Ito Y, Fukuda M, Kawashima H. 2010. Novel anti-carbohydrate antibodies reveal the cooperative function of sulfated N- and O-glycans in lymphocyte homing. *J Biol Chem*. 285:40864–40878.

Hiraoka N, Petryniak B, Kawashima H, Mitoma J, Akama TO, Fukuda MN, Lowe JB, Fukuda M. 2007. Significant decrease in alpha1,3-linked fucose in association with increase in 6-sulfated *N*-acetylglucosamine in peripheral lymph node addressin of FucT-VII-deficient mice exhibiting diminished lymphocyte homing. *Glycobiology.* 17:277–293.

Homeister JW, Thall AD, Petryniak B, Maly P, Rogers CE, Smith PL, Kelly RJ, Gersten KM, Askari SW, Cheng G, et al. 2001. The alpha(1,3)fucosyltransferases FucT-IV and FucT-VII exert collaborative control over selectin-dependent leukocyte recruitment and lymphocyte homing. *Immunity.* 15:115–126.

Honke K, Zhang Y, Cheng X, Kotani N, Taniguchi N. 2004. Biological roles of sulfoglycolipids and pathophysiology of their deficiency. *Glycoconj J*. 21:59–62.

Hosono-Fukao T, Ohtake-Niimi S, Nishitsuji K, Hossain MM, van Kuppevelt TH, Michikawa M, Uchimura K. 2011. RB4CD12 epitope expression and heparan sulfate disaccharide composition in brain vasculature. *J Neurosci Res*. 89:1840–1848.

Kawashima H, Petryniak B, Hiraoka N, Mitoma J, Huckaby V, Nakayama J, Uchimura K, Kadomatsu K, Muramatsu T, Lowe JB, et al. 2005. *N*-acetylglucosamine-6-*O*-sulfotransferases 1 and 2 cooperatively control lymphocyte homing through L-selectin ligand biosynthesis in high endothelial venules. *Nat Immunol*. 6:1096–1104.

Khoo KH, Yu SY. 2010. Mass spectrometric analysis of sulfated N- and O-glycans. *Methods Enzymol*. 478:3–26.

Kimura N, Ohmori K, Miyazaki K, Izawa M, Matsuzaki Y, Yasuda Y, Takematsu H, Kozutsumi Y, Moriyama A, Kannagi R. 2007. Human B-lymphocytes express alpha2–6-sialylated 6-sulfo-*N*-acetyllactosamine serving as a preferred ligand for CD22/Siglec-2. *J Biol Chem*. 282:32200–32207.

Koenig A, Jain R, Vig R, Norgard-Sumnicht KE, Matta KL, Varki A. 1997. Selectin inhibition: Synthesis and evaluation of novel sialylated, sulfated and fucosylated oligosaccharides, including the major capping group of GlyCAM-1. *Glycobiology*. 7:79–93.

Ley K, Laudanna C, Cybulsky MI, Nourshargh S. 2007. Getting to the site of inflammation: The leukocyte adhesion cascade updated. *Nat Rev Immunol*. 7:678–689.

Li X, Tu L, Murphy PG, Kadono T, Steeber DA, Tedder TF. 2001. CHST1 and CHST2 sulfotransferase expression by vascular endothelial cells regulates shear-resistant leukocyte rolling via L-selectin. *J Leukoc Biol*. 69:565–574.

Mehmet H, Scudder P, Tang PW, Hounsell EF, Caterson B, Feizi T. 1986. The antigenic determinants recognized by three monoclonal antibodies to keratan sulphate involve sulphated hepta- or larger oligosaccharides of the poly(*N*-acetyllactosamine) series. *Eur J Biochem*. 157:385–391.

Mitoma J, Bao X, Petryanik B, Schaerli P, Gauguet JM, Yu SY, Kawashima H, Saito H, Ohtsubo K, Marth JD, et al. 2007. Critical functions of N-glycans in L-selectin-mediated lymphocyte homing and recruitment. *Nat Immunol*. 8:409–418.

Mitsuoka C, Sawada-Kasugai M, Ando-Furui K, Izawa M, Nakanishi H, Nakamura S, Ishida H, Kiso M, Kannagi R. 1998. Identification of a major carbohydrate capping group of the L-selectin ligand on high endothelial venules in human lymph nodes as 6-sulfo sialyl Lewis X. *J Biol Chem*. 273:11225–11233.

Miyazaki K, Sakuma K, Kawamura YI, Izawa M, Ohmori K, Mitsuki M, Yamaji T, Hashimoto Y, Suzuki A, Saito Y, et al. 2012. Colonic epithelial cells express specific ligands for mucosal macrophage immunosuppressive receptors siglec-7 and -9. *J Immunol*. 188:4690–4700.

Ng TF, Streilein JW. 2001. Light-induced migration of retinal microglia into the subretinal space. *Invest Ophthalmol Vis Sci*. 42:3301–3310.

Nielsen JS, McNagny KM. 2009. The role of podocalyxin in health and disease. *J Am Soc Nephrol*. 20:1669–1676.

Paulson JC, Macauley MS, Kawasaki N. 2012. Siglecs as sensors of self in innate and adaptive immune responses. *Ann N Y Acad Sci*. 1253:37–48.

Rosen SD. 2004. Ligands for L-selectin: Homing, inflammation− beyond. *Annu Rev Immunol*. 22:129–156.

Satomaa T, Renkonen O, Helin J, Kirveskari J, Makitie A, Renkonen R. 2002. O-glycans on human high endothelial CD34 putatively participating in L-selectin recognition. *Blood*. 99:2609–2611.

Shibata TK, Matsumura F, Wang P, Yu S, Chou CC, Khoo KH, Kitayama K, Akama TO, Sugihara K, Kanayama N, et al. 2012. Identification of mono- and disulfated *N*-acetyl-lactosaminyl oligosaccharide structures as epitopes specifically recognized by humanized monoclonal antibody HMOCC-1 raised against ovarian cancer. *J Biol Chem*. 287:6592–6602.

Su AI, Wiltshire T, Batalov S, Lapp H, Ching KA, Block D, Zhang J, Soden R, Hayakawa M, Kreiman G, et al. 2004. A gene atlas of the mouse and human protein-encoding transcriptomes. *Proc Natl Acad Sci USA*. 101:6062–6067.

Tangemann K, Bistrup A, Hemmerich S, Rosen SD. 1999. Sulfation of a high endothelial venule-expressed ligand for L-selectin. Effects on tethering and rolling of lymphocytes. *J Exp Med*. 190:935–942.

Tateno H, Crocker PR, Paulson JC. 2005. Mouse Siglec-F and human Siglec-8 are functionally convergent paralogs that are selectively expressed on eosinophils and recognize 6′-sulfo-sialyl Lewis X as a preferred glycan ligand. *Glycobiology*. 15:1125–1135.

Tateno H, Ohnishi K, Yabe R, Hayatsu N, Sato T, Takeya M, Narimatsu H, Hirabayashi J. 2010. Dual specificity of Langerin to sulfated and mannosylated glycans via a single C-type carbohydrate recognition domain. *J Biol Chem*. 285:6390–6400.

Torii T, Fukuta M, Habuchi O. 2000. Sulfation of sialyl *N*-acetyllactosamine oligosaccharides and fetuin oligosaccharides by keratan sulfate Gal-6-sulfotransferase. *Glycobiology*. 10:203–211.

Uchimura K, Gauguet JM, Singer MS, Tsay D, Kannagi R, Muramatsu T, von Andrian UH, Rosen SD. 2005. A major class of L-selectin ligands is eliminated in mice deficient in two sulfotransferases expressed in high endothelial venules. *Nat Immunol*. 6:1105–1113.

Uchimura K, Kadomatsu K, Nishimura H, Muramatsu H, Nakamura E, Kurosawa N, Habuchi O, El-Fasakhany FM, Yoshikai Y, Muramatsu T. 2002. Functional analysis of the chondroitin 6-sulfotransferase gene in relation to lymphocyte subpopulations, brain development, and oversulfated chondroitin sulfates. *J Biol Chem*. 277:1443–1450.

Valenzuela DM, Murphy AJ, Frendewey D, Gale NW, Economides AN, Auerbach W, Poueymirou WT, Adams NC, Rojas J, Yasenchak J, et al. 2003. High-throughput engineering of the mouse genome coupled with high-resolution expression analysis. *Nat Biotechnol*. 21:652–659.

Walker JA, Smith KG. 2008. CD22: An inhibitory enigma. *Immunology*. 123:314–325.

Yang WH, Nussbaum C, Grewal PK, Marth JD, Sperandio M. 2012. Coordinated roles of ST3Gal-VI and ST3Gal-IV sialyltransferases in the synthesis of selectin ligands. *Blood*. 120:1015–1026.

Yeh JC, Hiraoka N, Petryniak B, Nakayama J, Ellies LG, Rabuka D, Hindsgaul O, Marth JD, Lowe JB, Fukuda M. 2001. Novel sulfated lymphocyte homing receptors and their control by a Core1 extension beta 1,3-*N*-acetylglucosaminyltransferase. *Cell*. 105:957–969.

Yoshino K, Ohmoto H, Kondo N, Tsujishita H, Hiramatsu Y, Inoue Y, Kondo H. 1997. Studies on selectin blockers. 4. Structure-function relationships of sulfated sialyl Lewis X hexasaccharide ceramides toward E-, P-, and L-selectin binding. *J Med Chem*. 40:455–462.

Yu SY, Wu SW, Hsiao HH, Khoo KH. 2009. Enabling techniques and strategic workflow for sulfoglycomics based on mass spectrometry mapping and sequencing of permethylated sulfated glycans. *Glycobiology*. 19:1136–1149.

Zhang H, Muramatsu T, Murase A, Yuasa S, Uchimura K, Kadomatsu K. 2006. *N*-acetylglucosamine 6-*O*-sulfotransferase-1 is required for brain keratan sulfate biosynthesis and glial scar formation after brain injury. *Glycobiology*. 16:702–710.